JACS
JOURNAL OF THE AMERICAN CHEMICAL SOCIETY
Article
Cite This: J. Am. Chem. Soc. XXXX, XXX, XXX−XXX
pubs.acs.org/JACS

In Situ Formation of N-Heterocyclic Carbene-Bound Single-Molecule Junctions

Evan A. Doud,[†,⊥] Michael S. Inkpen,[‡,⊥] Giacomo Lovat,[‡] Enrique Montes,[§] Daniel W. Paley,[∥] Michael L. Steigerwald,[†] Héctor Vázquez,[*,§] Latha Venkataraman,[*,†,‡] and Xavier Roy[*,†]

[†]Department of Chemistry, [‡]Department of Applied Physics and Applied Mathematics, and [∥]Columbia Nano Initiative, Columbia University, New York, New York 10027, United States

[§]Institute of Physics, Academy of Sciences of the Czech Republic, Cukrovarnická 10, Prague 16200, Czech Republic

Supporting Information

ABSTRACT: Self-assembled monolayers (SAMs) formed using N-heterocyclic carbenes (NHCs) have recently emerged as thermally and chemically ultrastable alternatives to those formed from thiols. The rich chemistry and strong σ-donating ability of NHCs offer unique prospects for applications in nanoelectronics, sensing, and electrochemistry. Although stable in SAMs, free carbenes are notoriously reactive, making their electronic characterization challenging. Here we report the first investigation of electron transport across single NHC-bound molecules using the scanning tunneling microscope-based break junction (STM-BJ) technique. We develop a series of air-stable metal NHC complexes that can be electrochemically reduced in situ to form NHC−electrode contacts, enabling reliable single-molecule conductance measurements of NHCs under ambient conditions. Using this approach, we show that the conductance of an NHC depends on the identity of the single metal atom to which it is coordinated in the junction. Our observations are supported by density functional theory (DFT) calculations, which also firmly establish the contributions of the NHC linker to the junction transport characteristics. Our work demonstrates a powerful method to probe electron transfer across NHC−electrode interfaces; more generally, it opens the door to the exploitation of surface-bound NHCs in constructing novel, functionalized electrodes and/or nanoelectronic devices.

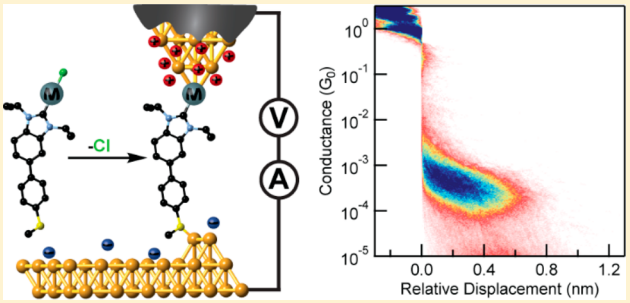

INTRODUCTION

A key design feature of nanoscale electronic devices is the chemical group that establishes the physical and electronic contact at the molecule−electrode interface. The nature of this interaction, i.e., covalent,[1−4] dative,[5] or supramolecular,[6] can be exploited to tune the stability and function of the connected component. One family of linkers with emerging potential are the carbenes, neutral molecules comprising a divalent carbon atom with a six-electron valence shell.[7] Originally considered too reactive to isolate, the development of stable, persistent carbenes such as N-heterocyclic carbenes (NHCs)[8] has played a critical role in many areas of modern chemistry.[9] While NHCs have been used extensively as tunable ligands for organometallic complexes, their ability to strongly bind nanoparticles or planar surfaces has only recently been recognized.[10] Johnson, Crudden, and their respective co-workers have demonstrated that NHCs can form self-assembled monolayers (SAMs) on Au that exhibit remarkable thermal and chemical stability;[11−13] NHCs in solution are even capable of rapidly displacing preformed thiol−Au SAMs.[12] Given their strong σ-donor binding to metals and unique electronic structure,[9] this family of molecules offers exciting new prospects for surface functionalization, with potential applications in selective heterogeneous catalysis,[14−17] nanotechnology,[10,18,19] and sensing.[10,11,13,20] Essential to such developments is an improved understanding of both the electronic coupling between the carbene and the metal surface and the electron transport across the carbene−electrode interface. Despite theoretical interest,[21,22] these features have never been experimentally investigated.

In this work, we describe a novel strategy to probe the electronic properties of NHCs on Au electrodes. Using the scanning tunneling microscope-based break junction (STM-BJ) technique,[2,23] we form NHC−electrode contacts via in situ electrochemical conversion of a metal NHC complex in the junction (Figure 1a). By measuring the electrical transport properties of a series of NHC-bound single-molecule junctions, we find that the conductance (G) of the junction depends on the metal atom in the precursor. Our hypothesis, supported by transport calculations based on density functional theory (DFT), is that as the complex is reduced at the STM tip the NHC remains coordinated to the metal atom. This atom subsequently binds to the electrode surface and establishes a conductive contact. By extending the backbone of the NHC-bound single-molecule junction, we observe a clear exponential

Received: May 17, 2018

DOI: 10.1021/jacs.8b05184
J. Am. Chem. Soc. XXXX, XXX, XXX−XXX

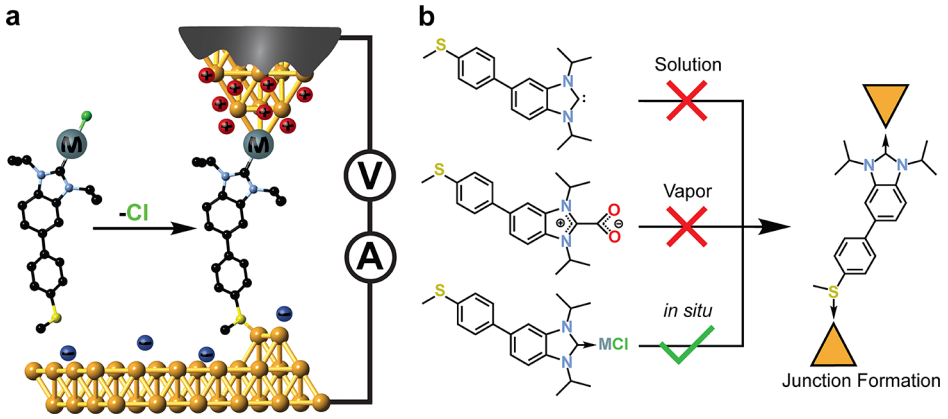

Figure 1. (a) Schematic of an NHC-bound single-molecule junction created via in situ electrochemical conversion of a metal NHC complex. (b) Synthetic strategies employed to prepare NHC-bound SAMs for subsequent STM-BJ measurements in air (solution, vapor). These proved unsuccessful, in contrast to the use of metal NHC complexes to form junctions directly from solution (in situ).

decay of conductance, indicating a coherent nonresonant transport mechanism. These results establish our approach as a robust yet flexible strategy to form NHC-linked molecular junctions.

EXPERIMENTAL SECTION

STM-BJ Details. Conductance measurements were carried out using the STM-BJ technique, which has been described in detail elsewhere.[23] Conductance measurements for all complexes were performed using 10 μM solutions in PC. The Au tip was coated with an insulating layer to suppress background ionic current. The insulated tips were created by driving a mechanically cut gold tip through Apiezon wax.[24] 1D conductance histograms were constructed using logarithmic bins (100 per decade) without any data selection.

Synthesis of NHC1−AuCl. The **NHC1−AuCl** complex was synthesized using a modified literature procedure.[25] **NHC1−HI** (45 mg, 100 μmol; synthesis detail in Supporting Information) was suspended in 8 mL of THF. KO^{t}Bu (12 mg, 110 μmol) was added to the suspension, and the reaction was stirred for 1 h. The mixture was then filtered through Celite, and $(SMe)_2AuCl$ (31 mg, 105 μmol) was added to the filtrate. The reaction was stirred for 3 h, protected from light. Activated carbon (~100 mg) was added to the reaction, which was stirred for 1 h and then filtered through Celite. The solvent was then removed in vacuo. The solid residue was redissolved in DCM and filtered, and the solvent was removed in vacuo to yield the pure complex **NHC1−AuCl** as a light-yellow powder (yield = 48 mg, 86%). Analogous procedures were used to prepare the other **NHC*n*−MCl** complexes.

Computational Details. The electronic and transport properties of molecular junctions were calculated using first-principles methods based on DFT-NEGF.[26,27] We modeled the junction by attaching the molecular backbone on the carbene side to an Au adatom for **NHC*n*−AuCl**, an Ag adatom for **NHC1−AgCl**, and a Cu adatom for **NHC1−CuCl** (without including the Cl atom). To simplify geometry optimization, the isopropyl groups were replaced with methyl groups, resulting in negligible changes in conductance. The SMe side was attached to an Au adatom for all junctions. The supramolecular structure was placed between two electrodes that consisted of a 4 × 4 face-centered cubic (fcc) Au(111) surface. We optimized the junction structure by relaxing the coordinates of the molecular backbone and the Au atoms to a force threshold smaller than 0.02 eV/Å, also optimizing the interelectrode vertical separation. In the calculations, the exchange correlation was described using the GGA approximation in the PBE implementation.[28] We used a double-ζ polarized local-orbital basis for molecular atoms and a single-ζ basis for Au atoms. We performed subsequent transport calculations at optimized geometries by adding additional Au(111) layers. We used Monkhorst−Pack grids of 5 × 5 × 1 and 15 × 15 × 1 for calculating the electronic structure and transmission spectra, respectively. Transmission eigenchannels were computed at the center of the Brillouin zone.[29]

RESULTS AND DISCUSSION

Our first objective was to measure the transport properties of a linear aromatic molecule utilizing an NHC as the contacting group. To achieve this goal, we exploited a new in situ electrochemical-reduction approach to form the single-molecule junction using the STM-BJ technique (Figure 1a). For this method, the molecule is terminated by an aurophilic thiomethyl group (SMe) on one end and a benzannulated NHC on the other end. The NHC is capped with one of a series of metal chloride complexes; the resulting air-stable metal NHC precursors are labeled **NHC1−MCl** (**M** = Au, Ag, Cu). Synthetic details are included in the Experimental Section. A single-molecule junction is established when the SMe binds to the electrode surface via an Au−S bond, and the metal NHC complex is reduced at the STM tip. We have developed this innovative strategy because we were unable to characterize the single-molecule transport characteristics of NHCs bound in SAMs prepared using traditional methods, shown in Figure 1b. Indeed, STM-BJ measurements of monolayers assembled on Au surfaces from solutions of free NHCs, or from the vapor phase using NHC−CO_2 adduct precursors,[12,30] did not yield reproducible conductance results.

Figure 2a presents the molecular structure of the precursors **NHC1−CuCl**, **NHC1−AgCl**, and **NHC1−AuCl**, as determined by single-crystal X-ray diffraction (SCXRD). Details of the STM-BJ measurements in an ionic environment have been described previously[31] and are outlined in the Experimental Section. Briefly, the measurements are performed using an insulated Au STM tip, with an exposed area of ~1 μm^2, and an Au substrate with an area larger than 1 cm^2. When a bias is applied, a dense double layer of charge builds up around the small area of the coated tip while a sparse double layer is formed on the large-area, uncoated substrate. Previous studies have demonstrated that, under these conditions, redox-active compounds such as ferrocene[32] or molecular clusters[33] can be oxidized or reduced in the junction under positive or negative tip biases, respectively.

When we use this approach with **NHC1−MCl** in propylene carbonate (PC), we can form electrically conducting NHC-bound single-molecule junctions by applying a negative (i.e.,

DOI: 10.1021/jacs.8b05184
J. Am. Chem. Soc. XXXX, XXX, XXX−XXX

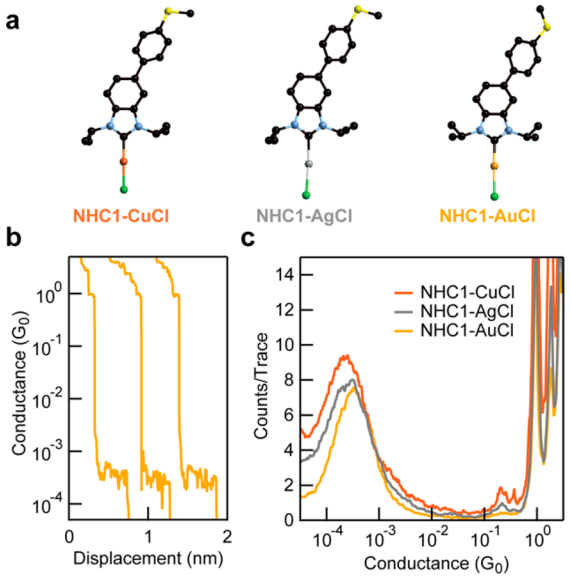

Figure 2. (a) Molecular structure of **NHC1−MCl**, as determined by SCXRD. Color code: black, C; blue, N; yellow, S; green, Cl; orange, Cu; gray, Ag; gold, Au. Hydrogens are omitted. (b) Sample conductance versus displacement traces of **NHC1−AuCl**, offset laterally for clarity. The plateau at $\sim 3 \times 10^{-4}$ G_0 results from the single-molecule junction. (c) Logarithmically binned 1D conductance histograms (100 bins/decade) of **NHC1−MCl** junctions, each composed of at least 2 000 traces without data selection. All measurements are in PC at a tip bias of −720 mV.

reducing) tip bias. Figure 2b shows sample conductance versus displacement traces for **NHC1−AuCl**, measured under a reducing tip bias of −720 mV. Clear conductance plateaus are visible at $\sim 3 \times 10^{-4}$ G_0 ($G_0 = 2e^2/h$ is the quantum of conductance), which we attribute to the conductance of the NHC-bound single-molecule junction. These measurements are repeated thousands of times, and the traces are compiled into logarithmically binned one-dimensional (1D) histograms, without data selection. Figure 2c presents the 1D histograms of all three **NHC1−MCl** complexes measured at −720 mV tip bias. Each histogram shows peaks close to integer multiples of G_0, indicating the formation of Au point contacts, as well as a peak between 10^{-4} and 10^{-3} G_0, corresponding to the most probable conductance of the NHC-bound single-molecule junction. Remarkably, we find that the position of the conductance peak depends on the metal in the precursor and decreases across the series as Au > Ag > Cu.

We emphasize that the NHC-bound junctions form reproducibly under negative (reductive) tip bias but not under positive (oxidative) tip bias (Figure S8). This strongly suggests that, through the application of a negative tip bias, the metal complex in the junction is reduced and binds to the electrode, that is, **NHC1**−$M^{I}Cl$ → **NHC1**−M^{0}−electrode. In addition to the bias polarity dependence, this hypothesis is supported by several observations and control experiments. (1) The metal-dependent conductance values indicate that the NHC group remains coordinated to the precursor metal atom even as it is reduced and binds to the electrode (Figure 2c). (2) The in situ formation of molecule−electrode bonds has previously been reported using benzyltrialkylstannane and benzyl−Au(PPh_3) contact group precursors.[3] (3) We synthesized two complexes as controls and measured their single-molecule conductance (Figures S9a and b). The first complex, [**NHC1−AuPPh$_3$**][**BF$_4$**], is analogous to **NHC1−AuCl**, but the Cl^- ligand is replaced with a weakly coordinating BF_4^- anion and PPh_3, which is known to dissociate from Au complexes upon junction formation.[3] The conductance of [**NHC1−AuPPh$_3$**][**BF$_4$**] is close to that of **NHC1−AuCl**, indicating that the molecular junction does not form by binding through the Cl atom to the Au electrode (i.e., **NHC1**−Au−Cl−electrode). The second complex, bis(diethyl(4-(methylthio)phenyl)phosphine)AuCl (((**4-MeSPh**)**Et$_2$P**)$_2$**AuCl**), is used to confirm that junctions formed via in situ reduction of gold chloride complexes are analogous to those formed by directly binding the free linker to the electrode. In this experiment, we replace the highly reactive NHC with a diethyl(aryl)phosphine group, which can be measured in the form of a metal chloride complex or as the free phosphine using the STM-BJ technique. In agreement with our premise, the conductance of the ((**4-MeSPh**)**Et$_2$P**)$_2$**AuCl** complex agrees well with that of the free phosphine.

To gain a deeper understanding of electron transport across the NHC−electrode interface, we investigate how the conductance of NHC-bound single-molecule junctions changes with increasing molecular length. For this, we synthesized a new series of asymmetric oligophenylene derivatives. As in the previous design, each molecule is terminated by a SMe group on one end and a benzannulated NHC−AuCl group on the other. Figure 3a shows the molecular structure of **NHC0−AuCl**, **NHC1−AuCl**, and

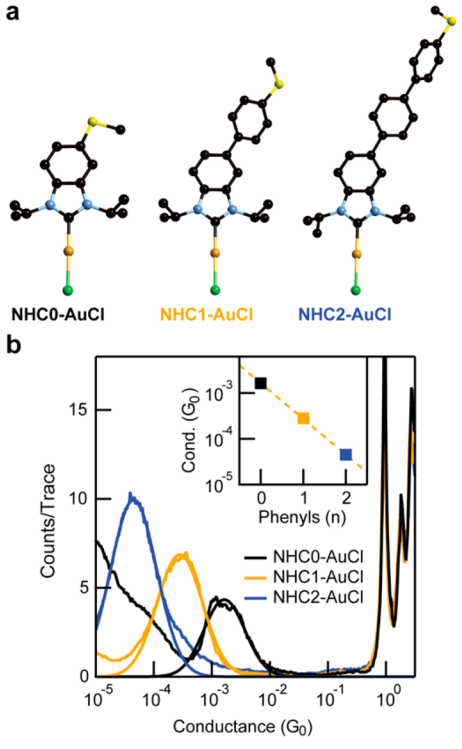

Figure 3. (a) Molecular structure of **NHC*n*−AuCl** (n = 0, 1, and 2), as determined by SCXRD. Note that the structure for **NHC1−AuCl** is repeated from Figure 2a for completeness. (b) Logarithmically binned 1D conductance histograms (100 bins/decade) of **NHC*n*−AuCl**, each composed of at least 2 000 traces obtained without data selection. All measurements are performed in PC at a tip bias of −360 mV. (Inset) Semilogarithmic plot of the conductance histogram peak value as a function of the number of phenylene units in the backbone of **NHC*n*−AuCl**.

DOI: 10.1021/jacs.8b05184
J. Am. Chem. Soc. XXXX, XXX, XXX−XXX

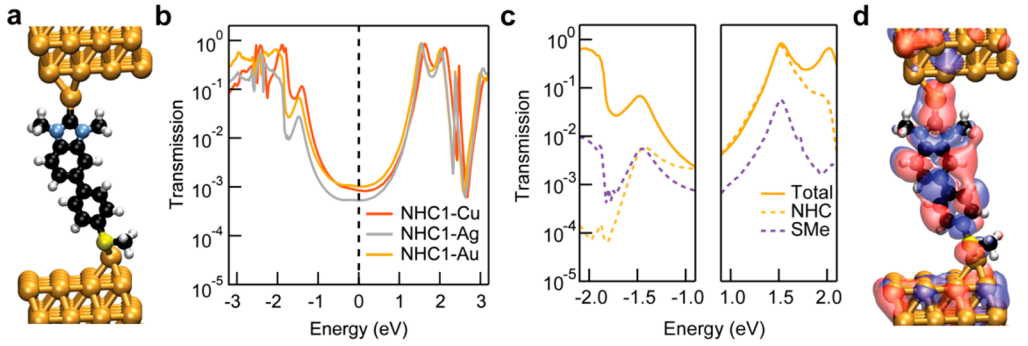

Figure 4. (a) Modeled structure of **NHC1−Au** junction. (b) Transmission function of **NHC1−M** junctions. (c) Projection of the electronic coupling matrices at the NHC and SMe contacts for the **NHC1−Au** junction onto the highest occupied molecular orbital (HOMO) (left) and lowest unoccupied molecular orbital (LUMO) (right). (d) Real-space representation of the most conducting transmission eigenchannel of **NHC1−Au** junction at the LUMO energy.

NHC2−AuCl, as determined by SCXRD. As with the **NHC1−MCl** series, molecular junctions only form under reducing conditions in PC. Figure 3b presents the 1D conductance histograms of all three molecules (2D conductance−displacement histograms are presented in Figure S10). Each histogram shows a clear peak below G_0, and the conductance decreases with increasing molecular length. The inset of Figure 3b shows a semilogarithmic plot of the conductance values, obtained from a Gaussian fit to the histogram as a function of the number of phenylene units (n) in the molecular backbone. An exponential fit to the data with $G \sim e^{-\beta n}$ gives a conductance decay β = 1.8/phenylene. This β value is in good agreement with that reported for oligophenylene molecular junctions with other linkers.[2,34]

To support these measurements, we perform DFT-based atomistic calculations of **NHC1−M** and **NHC*n*−Au** junctions (see Experimental Section). These junctions are modeled with both NHC and SMe groups bound to undercoordinated metal atoms on the electrode surface (Figure 4a and Figure S11).[30,35] The atomic simulations underscore the strength of the NHC contact, regardless of the undercoordinated metal **M**: the computed binding energies of the NHC to the undercoordinated metal **M** are 1.6−2.0 eV (Table S2), comparable to reported binding energies of NHCs to Au(111) surfaces (1.5−1.75 eV),[12,30] and significantly higher than those calculated for thiolate-based Au−S bonds.[36,37] For the **NHC*n*−Au** series, the calculated binding energy of the molecule in the junction is ∼2.7 eV and is essentially independent of the number of phenylene units n (Table S2). The NHC contact is responsible for most of the binding (∼2.0 eV), while the contribution of the Au−SMe bond is smaller (∼0.7 eV), in agreement with previous calculations.[38]

DFT-based transport calculations are subsequently applied to establish the role the NHC contact plays in the transport properties of **NHC1−M** and **NHC*n*−Au** junctions. Figure 4b presents the calculated transmissions as a function of energy relative to Fermi level (E_F) for all three types of **NHC1−M** junction. For each junction type, the high-transmission peak closest to E_F derives from the lowest unoccupied molecular orbital (LUMO). A peak with lower transmission originating from a S-localized metal-molecule state is observed at ca. −1.5 V, which has previously been attributed to the Au−S gateway state.[39] The precursor metal atom **M** introduces only minor changes in the transmission function, but it modulates the low-bias conductance. In agreement with the measurements, we find a slightly lower conductance for Ag and Cu precursors than for Au. The position of the occupied resonance and resulting zero-bias conductance follow the trend in the position of the d-states in Au, Ag, and Cu.[40]

Analysis of the transmission functions of the **NHC*n*−Au** junctions reveal that the LUMO and other empty molecular states derive mainly from the NHC unit while the SMe group contributes to the occupied state around −1.5 eV (Figures S12 and S13). The computed conductance for the **NHC*n*−Au** junctions decreases exponentially as n increases. An exponential fit to the calculated values yields a decay constant $\beta \approx 1.6$/phenylene (Figure S14), slightly lower than the experimental β. This difference is in line with the general trends of DFT-based calculations.[27]

The projection of the electronic coupling matrices of the NHC/SMe contacts (top/bottom contacts in Figure 4a) for the **NHC1−Au** junction onto the HOMO and LUMO (Figure 4c) reveals the role the NHC plays in the transport characteristics (see Supporting Information for details). The low transmission observed when the NHC or SMe contacts are projected onto the HOMO (left panel in Figure 4c) illustrates the poor electronic coupling of this state to the electrodes. By contrast, when the coupling matrix of the NHC−Au contact is projected onto the (NHC-derived) LUMO, the total transmission is almost recovered (right panel in Figure 4c). This demonstrates the excellent conducting properties of the NHC linker and quantifies the electronic coupling of the NHC-derived state to the electrode. In agreement with this finding, we see that current is carried by a single transmission channel, shown in Figure 4d at the LUMO energy, which resembles the LUMO of the isolated molecule (see Figure S15).

CONCLUSION

By designing a series of metal NHC complexes that can be electrochemically reduced in situ at the STM tip to form the NHC−electrode contact, we have demonstrated the first single-molecule study of electron transfer across an NHC−metal interface. Experimental and theoretical data indicate that the NHC conducts primarily through the LUMO. Given that many types of carbenes can form stable metal complexes, our in situ electrochemical approach opens the door to exploring the electronic properties of a wide range of carbene−electrode interfaces beyond NHCs. Remarkably, our method also introduces a unique strategy to manipulate the conductance of a single-molecule junction through in situ formation of heterometallic electrode contacts. Our results thus chart a clear path to define the final electrode structure down to the atomic

DOI: 10.1021/jacs.8b05184
J. Am. Chem. Soc. XXXX, XXX, XXX−XXX

level, through a combination of careful molecular design and synthetic electrochemistry.

■ ASSOCIATED CONTENT

Supporting Information

The Supporting Information is available free of charge on the ACS Publications website at DOI: 10.1021/jacs.8b05184.

Additional data, synthetic methods, and characterization (PDF)
$C_{14}H_{20}AuClN_2S$ (CIF)
$C_{20}H_{24}AuClN_2S$ (CIF)
$C_{26}H_{28}AuClN_2S$ (CIF)
$C_{40}H_{48}Ag_2Cl_2N_4S_2$ (CIF)
$C_{20}H_{24}ClCuN_2S$ (CIF)
$C_{22}H_{34}AuClP_2S_2$ (CIF)

■ AUTHOR INFORMATION

Corresponding Authors

*vazquez@fzu.cz
*lv2117@columbia.edu
*xr2114@columbia.edu

ORCID

Giacomo Lovat: 0000-0001-8926-005X
Héctor Vázquez: 0000-0002-3865-9922
Latha Venkataraman: 0000-0002-6957-6089
Xavier Roy: 0000-0002-8850-0725

Author Contributions

⊥E.A.D. and M.S.I. contributed equally to this work.

Notes

The authors declare no competing financial interest.

■ ACKNOWLEDGMENTS

We are grateful to N. R. Papior for useful discussion. This work was supported in part by the Center for Precision Assembly of Superstratic and Superatomic Solids at Columbia University, an NSF MRSEC (DMR-1420634). Acknowledgment is made to the Donors of the American Chemical Society Petroleum Research Fund for partial support of this research (ACS PRF no. 57062-DNI10). Part of this work was also supported by the U.S. Air Force Office of Scientific Research (AFOSR) Grant no. FA9550-18-1-0020. Single-crystal X-ray diffraction analysis was performed at the Shared Materials Characterisation Laboratory (SMCL) at Columbia University. Use of the SMCL was made possible by funding from Columbia University. E.M. and H.V. thank the Purkyně Fellowship program of the Czech Academy of Sciences and the Czech Science Foundation (15-19672S). Computational resources were provided by the National Grid Infrastructure MetaCentrum and the "Projects of Large Research, Development, and Innovations Infrastructures" program (CESNET LM2015042 and LM2015087). M.S.I. was supported primarily by a Marie Skłodowska Curie Global Fellowship (MOLCLICK: 657247) within the Horizon 2020 Program.

■ REFERENCES

(1) Reed, M. A.; Zhou, C.; Muller, C. J.; Burgin, T. P.; Tour, J. M. *Science* **1997**, *278*, 252−254.
(2) Xu, B.; Tao, N. J. *Science* **2003**, *301*, 1221−1223.
(3) Cheng, Z. L.; Skouta, R.; Vazquez, H.; Widawsky, J. R.; Schneebeli, S.; Chen, W.; Hybertsen, M. S.; Breslow, R.; Venkataraman, L. *Nat. Nanotechnol.* **2011**, *6*, 353−357.
(4) Zang, Y.; Pinkard, A.; Liu, Z.-F.; Neaton, J. B.; Steigerwald, M. L.; Roy, X.; Venkataraman, L. *J. Am. Chem. Soc.* **2017**, *139*, 14845−14848.
(5) Park, Y. S.; Whalley, A. C.; Kamenetska, M.; Steigerwald, M. L.; Hybertsen, M. S.; Nuckolls, C.; Venkataraman, L. *J. Am. Chem. Soc.* **2007**, *129*, 15768−15769.
(6) Martin, C. A.; Ding, D.; Sorensen, J. K.; Bjornholm, T.; van Ruitenbeek, J. M.; van der Zant, H. S. J. *J. Am. Chem. Soc.* **2008**, *130*, 13198−13199.
(7) Bourissou, D.; Guerret, O.; Gabbai, F. P.; Bertrand, G. *Chem. Rev.* **2000**, *100*, 39−92.
(8) Arduengo, A. J.; Harlow, R. L.; Kline, M. *J. Am. Chem. Soc.* **1991**, *113*, 361−363.
(9) Hopkinson, M. N.; Richter, C.; Schedler, M.; Glorius, F. *Nature* **2014**, *510*, 485−496.
(10) Zhukhovitskiy, A. V.; MacLeod, M. J.; Johnson, J. A. *Chem. Rev.* **2015**, *115*, 11503−11532.
(11) Zhukhovitskiy, A. V.; Mavros, M. G.; Van Voorhis, T.; Johnson, J. A. *J. Am. Chem. Soc.* **2013**, *135*, 7418−7421.
(12) Crudden, C. M.; Horton, J. H.; Ebralidze, II; Zenkina, O. V.; McLean, A. B.; Drevniok, B.; She, Z.; Kraatz, H. B.; Mosey, N. J.; Seki, T.; Keske, E. C.; Leake, J. D.; Rousina-Webb, A.; Wu, G. *Nat. Chem.* **2014**, *6*, 409−414.
(13) Crudden, C. M.; Horton, J. H.; Narouz, M. R.; Li, Z.; Smith, C. A.; Munro, K.; Baddeley, C. J.; Larrea, C. R.; Drevniok, B.; Thanabalasingam, B.; McLean, A. B.; Zenkina, O. V.; Ebralidze, I. I.; She, Z.; Kraatz, H.-B.; Mosey, N. J.; Saunders, L. N.; Yagi, A. *Nat. Commun.* **2016**, *7*, 12654.
(14) Herrmann, W. A.; Elison, M.; Fischer, J.; Köcher, C.; Artus, G. R. J. *Angew. Chem., Int. Ed. Engl.* **1995**, *34*, 2371−2374.
(15) Vougioukalakis, G. C.; Grubbs, R. H. *Chem. Rev.* **2010**, *110*, 1746−1787.
(16) Fortman, G. C.; Nolan, S. P. *Chem. Soc. Rev.* **2011**, *40*, 5151−5169.
(17) Huynh, H. V. *The Organometallic Chemistry of N-Heterocyclic Carbenes*; John Wiley & Sons, Inc.: Hoboken, NJ, 2017.
(18) Ott, L. S.; Cline, M. L.; Deetlefs, M.; Seddon, K. R.; Finke, R. G. *J. Am. Chem. Soc.* **2005**, *127*, 5758−5759.
(19) Hurst, E. C.; Wilson, K.; Fairlamb, I. J. S.; Chechik, V. *New J. Chem.* **2009**, *33*, 1837−1840.
(20) Weidner, T.; Baio, J. E.; Mundstock, A.; Große, C.; Karthäuser, S.; Bruhn, C.; Siemeling, U. *Aust. J. Chem.* **2011**, *64*, 1177−1179.
(21) Foti, G.; Vázquez, H. *Nanotechnology* **2016**, *27*, 125702.
(22) Kim, H. K.; Hyla, A. S.; Winget, P.; Li, H.; Wyss, C. M.; Jordan, A. J.; Larrain, F. A.; Sadighi, J. P.; Fuentes-Hernandez, C.; Kippelen, B.; Brédas, J.-L.; Barlow, S.; Marder, S. R. *Chem. Mater.* **2017**, *29*, 3403−3411.
(23) Venkataraman, L.; Klare, J. E.; Nuckolls, C.; Hybertsen, M. S.; Steigerwald, M. L. *Nature* **2006**, *442*, 904−907.
(24) Nagahara, L. A.; Thundat, T.; Lindsay, S. M. *Rev. Sci. Instrum.* **1989**, *60*, 3128−3130.
(25) Gonell, S.; Poyatos, M.; Peris, E. *Angew. Chem., Int. Ed.* **2013**, *52*, 7009−7013.
(26) Soler, J. M.; Artacho, E.; Gale, J. D.; Garcia, A.; Junquera, J.; Ordejon, P.; Sanchez-Portal, D. *J. Phys.: Condens. Matter* **2002**, *14*, 2745−2779.
(27) Papior, N.; Lorente, N.; Frederiksen, T.; Garcia, A.; Brandbyge, M. *Comput. Phys. Commun.* **2017**, *212*, 8−24.
(28) Perdew, J. P.; Burke, K.; Ernzerhof, M. *Phys. Rev. Lett.* **1996**, *77*, 3865−3868.
(29) Paulsson, M.; Brandbyge, M. *Phys. Rev. B: Condens. Matter Mater. Phys.* **2007**, *76*, 115117.
(30) Wang, G.; Ruhling, A.; Amirjalayer, S.; Knor, M.; Ernst, J. B.; Richter, C.; Gao, H. J.; Timmer, A.; Gao, H. Y.; Doltsinis, N. L.; Glorius, F.; Fuchs, H. *Nat. Chem.* **2017**, *9*, 152−156.
(31) Capozzi, B.; Chen, Q.; Darancet, P.; Kotiuga, M.; Buzzeo, M.; Neaton, J. B.; Nuckolls, C.; Venkataraman, L. *Nano Lett.* **2014**, *14*, 1400−1404.

DOI: 10.1021/jacs.8b05184
J. Am. Chem. Soc. XXXX, XXX, XXX−XXX

(32) Capozzi, B.; Xia, J. L.; Adak, O.; Dell, E. J.; Liu, Z. F.; Taylor, J. C.; Neaton, J. B.; Campos, L. M.; Venkataraman, L. *Nat. Nanotechnol.* **2015**, *10*, 522−527.
(33) Lovat, G.; Choi, B.; Paley, D. W.; Steigerwald, M. L.; Venkataraman, L.; Roy, X. *Nat. Nanotechnol.* **2017**, *12*, 1050−1054.
(34) Quek, S. Y.; Choi, H. J.; Louie, S. G.; Neaton, J. B. *Nano Lett.* **2009**, *9*, 3949−3953.
(35) Kamenetska, M.; Koentopp, M.; Whalley, A. C.; Park, Y. S.; Steigerwald, M. L.; Nuckolls, C.; Hybertsen, M. S.; Venkataraman, L. *Phys. Rev. Lett.* **2009**, *102*, 126803.
(36) Lavrich, D. J.; Wetterer, S. M.; Bernasek, S. L.; Scoles, G. *J. Phys. Chem. B* **1998**, *102*, 3456−3465.
(37) Pontes, R. B.; Novaes, F. D.; Fazzio, A.; da Silva, A. J. R. *J. Am. Chem. Soc.* **2006**, *128*, 8996−8997.
(38) Hybertsen, M. S.; Venkataraman, L. *Acc. Chem. Res.* **2016**, *49*, 452−460.
(39) Vazquez, H.; Skouta, R.; Schneebeli, S.; Kamenetska, M.; Breslow, R.; Venkataraman, L.; Hybertsen, M. S. *Nat. Nanotechnol.* **2012**, *7*, 663−667.
(40) Hammer, B.; Morikawa, Y.; Norskov, J. K. *Phys. Rev. Lett.* **1996**, *76*, 2141−2144.

DOI: 10.1021/jacs.8b05184
J. Am. Chem. Soc. XXXX, XXX, XXX−XXX